PAPER

Primary damage in tungsten using the binary collision approximation, molecular dynamic simulations and the density functional theory

To cite this article: A De Backer *et al* 2016 *Phys. Scr.* **2016** 014018

IOP Publishing | Royal Swedish Academy of Sciences Physica Scripta

Phys. Scr. **T167** (2016) 014018 (7pp) doi:10.1088/0031-8949/T167/1/014018

Primary damage in tungsten using the binary collision approximation, molecular dynamic simulations and the density functional theory

A De Backer[1], A Sand[2], C J Ortiz[3], C Domain[4], P Olsson[5], E Berthod[6] and C S Becquart[6]

[1] CCFE, Culham Centre for fusion Energy, Abingdon, Oxon OX14 3DB, UK
[2] Department of Physics, University of Helsinki, PO Box 43, FI-00014 Helsinki, Finland
[3] Laboratorio Nacional de Fusión por Confinamiento Magnético, Av. Complutense 40, Madrid, Spain
[4] EDF Lab Les Renardieres, Dpt MMC, F-77250 Moret sur Loing, France
[5] KTH Royal Institute of Technology, Reactor Physics, Roslagstullsbacken 21, SE-10691 Stockholm, Sweden
[6] UMET, UMR 8207, Université Lille I, F-59655 Villeneuve d'Ascq cédex, France

E-mail: andree.debacker@ccfe.ac.uk

Received 26 May 2015, revised 7 October 2015
Accepted for publication 15 October 2015
Published 12 January 2016

Abstract

The damage produced by primary knock-on atoms (PKA) in W has been investigated from the threshold displacement energy (TDE) where it produces one self interstitial atom–vacancy pair to larger energies, up to 100 keV, where a large molten volume is formed. The TDE has been determined in different crystal directions using the Born–Oppenheimer density functional molecular dynamics (DFT-MD). A significant difference has been observed without and with the semi-core electrons. Classical MD has been used with two different empirical potentials characterized as 'soft' and 'hard' to obtain statistics on TDEs. Cascades of larger energy have been calculated, with these potentials, using a model that accounts for electronic losses (Sand *et al* 2013 *Europhys. Lett.* **103** 46003). Two other sets of cascades have been produced using the binary collision approximation (BCA): a Monte Carlo BCA using SDTrimSP (Eckstein *et al* 2011 *SDTrimSP: Version 5.00*. Report IPP 12/8) (similar to SRIM www.srim.org) and MARLOWE (RSICC Home Page. (https://rsicc.ornl.gov/codes/psr/psr1/psr-137.html) (accessed May, 2014)). The comparison of these sets of cascades gave a recombination distance equal to 12 Å which is significantly larger from the one we reported in Hou *et al* (2010 *J. Nucl. Mater.* **403** 89) because, here, we used bulk cascades rather than surface cascades which produce more defects (Stoller 2002 *J. Nucl. Mater.* **307** 935, Nordlund *et al* 1999 *Nature* **398** 49). Investigations on the defect clustering aspect showed that the difference between BCA and MD cascades is considerably reduced after the annealing of the cascade debris at 473 K using our Object Kinetic Monte Carlo model, LAKIMOCA (Domain *et al* 2004 *J. Nucl. Mater.* **335** 121).

Keywords: threshold displacement energy, recombination distance, binary collision approximation, DFT-MD

(Some figures may appear in colour only in the online journal)

1. Introduction

The evaluation of the damage produced by ions or neutrons usually uses models based on the binary collision approximation (BCA) or on molecular dynamics (MD) simulations. BCA based models are faster but require parameters such as threshold displacement energies or recombination radius. Full MD cascades are computer time consuming and rely on the development of empirical potentials. Furthermore, the damage evolves with time and temperature on multiple scales because of the mobility of the defects and their interactions and different techniques must be used. Given the short length of this paper we briefly describe the methods prior to the results. In the first section we present some results about the threshold displacement energies obtained by density functional (DFT-MD) and classic MD. The second section concerns the recombination distance that we determined by comparing BCA to MD cascades. In the last part, the defect cluster formation is briefly analyzed and preliminary results on the annealing of cascades using an OKMC are discussed.

2. Threshold displacement energies

DFT-MD simulations in the Born–Oppenheimer approximation have been performed over a large range of angles and knock-on energies in the micro-canonical (NVE) ensemble. The projector augmented wave (PAW) formalism [9, 10] has been applied in the generalized gradient approximation [11]. These methods are implemented in the Vienna *Ab initio* Simulation Package [12]. Non-cubic supercells of at least 648 bcc sites ($9 \times 6 \times 6$) have been used for the dynamic simulations. The DFT calculations were performed using two kinds of potentials: the minimal set regular PAW which considers 6s and 5d electrons as valence electrons and the semi-core PAW which also considers the 5p electrons. The minimal set regular PAW will be referred to as DFT, whereas the semi-core PAW will be referred to as DFT-sc. The time step used in the DFT-MD simulations was set from 1 to 2 fs depending on the primary knock-on atoms (PKA) energy, after some tests were performed. The simulation time was between 1 and 2 ps. All results here presented were obtained using the gamma point in the Brillouin zone and a cut-off energy of 230 eV.

As in our previous work in iron [13], to calculate threshold displacement energy (TDEs), one initiates a collision sequence along a specific direction, by giving the PKA, a kinetic energy, and more precisely a velocity along the direction chosen at 0 K. If at the end of the collision cascade no defect remains in the lattice, the PKA velocity is increased and a new simulation is launched. The TDE is the minimum at which a FP is observed at the end of the simulation.

For MD runs, one of Marinica *et al* potentials [14] has been interpolated to ZBL potential [15] in two different ways. They have been characterized as 'soft' (MS-s) and 'hard' (MS-h). For more statistics, 7000 MD runs 12 ps long were done in $12 \times 12 \times 16$ atom boxes as in [16], after 6 ps of thermalization at 36 K. From one run to another, the initial condition varies by the selection of the PKA among the eight atoms in the middle of the simulation box and the Miller indices of the exact lattice direction which are incrementally changed by 0.2.

Table 1. Threshold displacement energies (in eV) for the different cohesive models along different crystal orientation of BCC tungsten.

Orientation	DFT	DFT-sc	MS-s	MS-h
⟨100⟩	40	58	31	43
⟨110⟩	63	>80	51	71
⟨111⟩	44	>80	45	65

Table 1 gives the TDEs obtained by DFT-MD and MD methods. 'DFT' and 'DFT-sc' conditions gave TDE equal respectively to 40 eV and 58 eV in the ⟨100⟩ direction. Values for the ⟨110⟩ and ⟨111⟩ directions are larger. MD results are usually smaller than DFT and exhibit a broad distribution illustrated figure 1(a) for the ⟨100⟩ direction. As expected from its 'hard' character, MS-h predicts a larger TDE than MS-s and DFT-sc, a larger TDE than DFT. Another way of comparing these four cohesive models is by calculating the evolution of the energy increase when the initial atom is moved toward its nearest neighbor in a rigid lattice. This will be referred to as quasi static drag (QSD). QSD energy is showed for the ⟨100⟩ direction on figure 1(b). It appears clearly that the two conditions that predict higher energy threshold, i.e. DFT-sc and MS-h, exhibit a significantly higher QSD energy for distance ranging from 1 to 1.5 Å. The pair energy predicted by the ZBL potential is also reproduced which illustrates the difference in the interpolation of both empirical potentials. The DFT-sc condition is quite close to the ZBL potential. At equilibrium, the first nearest neighbor in the ⟨100⟩ direction is at 3.17 Å but during an MD simulation, an atom with large kinetic energy may come closer than 1.5 Å to its first nearest neighbor and the difference between the potentials at short distance will impact the energy transfer, the probability of FP formation and finally the resulting TDE. The TDEs correlate with the QSD energy when two atoms are separated by a distance of 1–2 Å: in DFT-MD and MD, the larger the energy, the larger the TDE.

In the simulations, we observed that, below the threshold energy, when the recombination takes place, it happens fast. Close to the threshold energy, the collision produces a vacancy and a crowdion which may have rotated. When they are at close distance from each other, the recombination is athermal and fast. At energy close to the threshold energy, the simulation outcome shows definitely variability, as demonstrated with the MD simulations. Typically, the two defects can be more distant and the recombination requires interactions with thermal fluctuations. For example, the rotation of the crowdion is a process that requires the overpass of an energetic barrier is the static lattice. Among others, a study of the recombination time as a function of the energy could be interesting and complete the comparison between DFT and MD simulations.

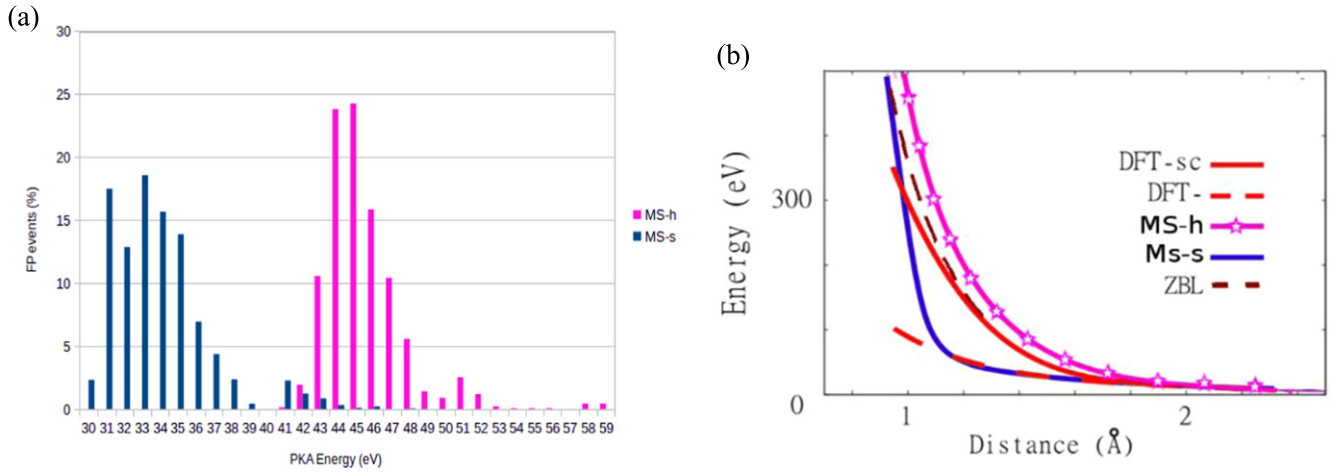

Figure 1. (a) Statistic of FP formed as a function of the PKA energy in the ⟨100⟩ direction in MD runs using the MS-h (hard) and MS-s (soft) empirical potentials; (b) energy increase when one atom is displaced toward its first nearest neighbor in the ⟨100⟩ direction with the different cohesive models.

3. The recombination distance

In this work, BCA and full classical MD cascades have been calculated for the same PKA energies, both models accounting for electronic losses. The BCA based models compute the development of cascade trajectories triggered by an energetic atom as a sequence of binary collisions rather than integrating the equations of motion of the whole system over time, as would be done with full classical MD.

The BCA has been combined with a Monte Carlo approach to model the cascade formation in slightly different models in SRIM [3] and SDTrimSP [2]. We used SDTrimSP whose model is detailed in [17]. The TDE, binding energy and cutoff energy are the main parameters of this model. In a first attempt, we used the concept of the TDE with an average value of 51 eV. In this approach, if the moving atom, which can be the initial projectile or one of the recoils, and the collided atom have a kinetic energy larger than the TDE, after the collision, a stable vacancy is considered to be formed. If both atoms stay with a kinetic energy smaller than the TDE, a self interstitial atom (SIA) is formed. If only the kinetic energy of the impinging atom is smaller than the TDE, a replacement collision occurs and in the opposite case the collision causes no defect.

Full cascade simulations were performed using PARCAS and MS-s and MS-h potentials for PKAs ranging from 1 to 100 keV. The simulations were performed at 0 K with periodic boundary conditions and random PKA directions. A Berendsen thermostat was applied to border atoms, to allow for heat transfer out of the cell, and to inhibit cascade self-interaction. Electronic stopping was included through the use of a friction term, applied to all atoms with a kinetic energy above 10 eV [1]. To analyze the MD cascades, a Wigner–Seitz (WS) analysis was done. The lattice is divided into WS cells and when one WS cell is empty, the coordinate of the cell is given as a vacant site.

The number of vacant sites as a function of time can be compared on figure 2 for 20 keV BCA and MD cascades. The

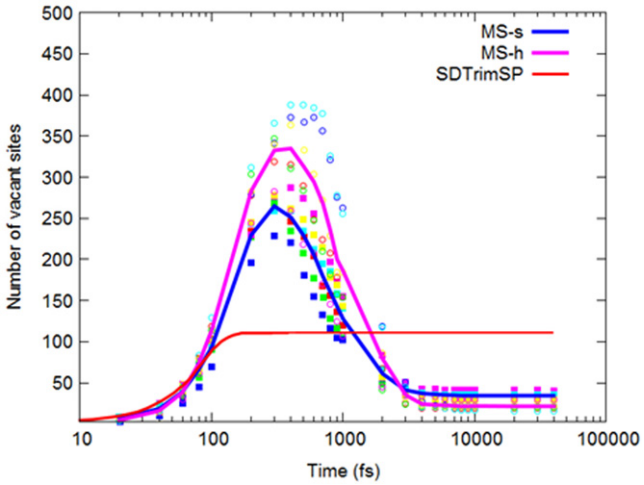

Figure 2. Number of vacant sites in 20 keV full classical MD and BCA cascades as a function of time.

calculations exhibit a similar evolution up to 100 fs. After that time, a plateau is reached in the BCA whereas full classical MD predicts 2–3 times more defects after 300–500 fs. The BCA simulations do not count for any recombination of vacancies and interstitials and with the threshold energy of 51 eV, it was not possible to reproduce the MD results (maximum number or final number of defects). It can be noticed that the softer potential predicted more vacant sites at the maximum. The cause is the lower energy transfer to the surrounding atoms which has two effects: (1) there are less 'vacancies' at peak damage because there is less of a heat spike, and (2) the weaker heat spike means less recombination at the later phase, resulting in more surviving defects. Also, since there is less energy transfer to surrounding atoms, the recoils themselves can travel further, which results in less in-cascade recombination.

We then used the concept of recombination distance as we did with MARLOWE [4, 5, 18]. MARLOWE is based on

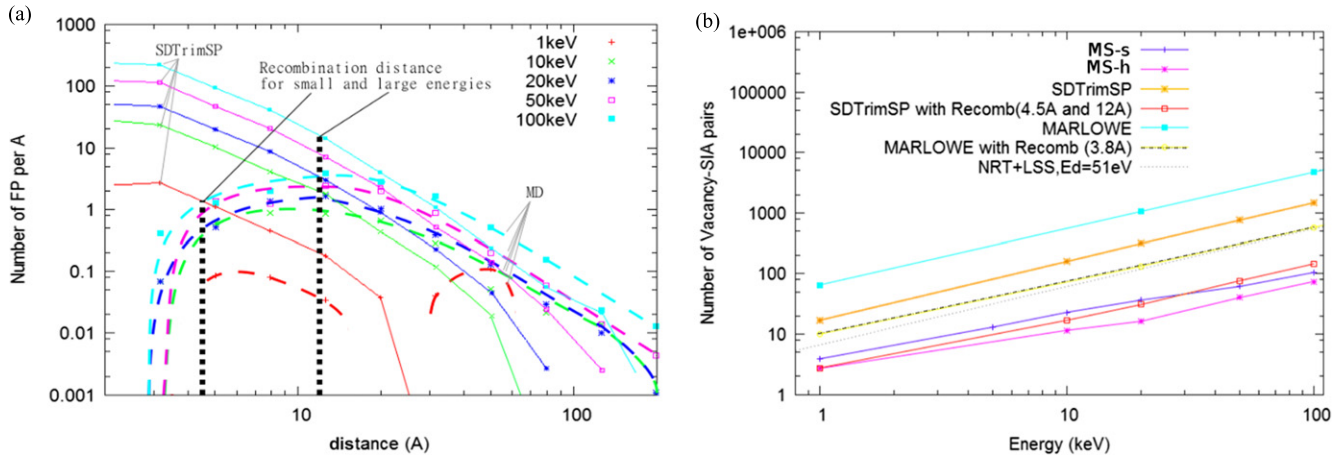

Figure 3. (a) Average distributions of SIA-vacancy pairs as a function of their mutual distance in SDTrimSP and full MD cascades with MS-s potential, for PKA energies ranging from 1 to 100 keV; (b) number of pairs of defects as a function of the PKA energy predicted by all the models.

the BCA and takes into account the crystalline structure of materials, which allows accounting for crystal lattice effects such as channeling and focusing chains that may influence trajectories and subsequent atomic displacements. An atom is displaced from its lattice site if the energy given by the projectile during the collision, is larger than its binding energy to the crystal. In the case of metals, the binding energy of a lattice atom corresponds to the cohesive energy. As SDTrimSP, MARLOWE does not account for long-range interactions between defects and cannot hence account for the recombination of SIAs and vacancies during the cascade. Our previous works [19, 20], motivated by the early MD simulations of subthreshold energy cascades of Scholz and Lehmann [21], showed that to some extent, it is possible to emulate, among others, the spontaneous recombination of SIA and vacancies that occurs during the thermal spike regime by considering a spherical volume capture between the defects. We used the same approach in this work and investigate the other sources of difference between BCA and MD approaches as well as consequences in long term simulations. Cascades obtained with MARLOWE were calculated using the ZBL potential [1] in the ⟨111⟩ direction for PKA energies of 1, 20, 100 and 400 keV. The binding energy was taken equal to 8.9 eV and the recombination distance was 1.2 a_0, where a_0 is tungsten lattice parameter.

With SDTrimSP, we mimicked this method by equaling the TDE to the binding energy. Many more defects are formed, in particular close defects, which do not exist in full classical MD cascades. After the cascade calculation, the vacancies and SIA are paired starting with the ones which are closest from each other and eliminated when they are less distant that the recombination distance. The recombination distance should be a unique value that leads to similar number of defects in BCA and MD cascades but both potential (MS-s) predicted different defect numbers. The soft potential gave in particular more SIA-vacancy pairs of small mutual distance. Furthermore to reproduce the full energy range of the MD results, two significantly different recombination radii need to be used. For the 1 keV cascades, a recombination radius equal to 4.5 Å which is close to the one we obtained in [5] provides agreement between MD and BCA, whereas for the larger energy cascades a much larger recombination radius close to 12 Å was necessary. The distributions of SIA-vacancy pairs as a function of their mutual distance in BCA and MD (with MS-s) cascades are plotted on figure 3(a). When the recombination distance is used the small distance part of the distribution is truncated however a deficit of small pairs and large pairs (70–200 Å) remains as well as an excess in between, compared to MD cascades.

Figure 3(b) shows the number of pairs of defects as a function of the PKA energy predicted by the different models. As expected, BCA models without the recombination distance overestimate this number and SDTrimSP with the recombination distance is close to MD. However MARLOWE, used with a recombination distance equal to 3.8 Å predicts 5–10 times more defects than MD. The discrepancy between the recombination distance obtained in our previous work and the one found here comes from the fact that here cascades have been simulated in the bulk, whereas it was surface cascades in our previous work [5]. In [6] a factor 2 between defects in cascades on surface and in bulk is reported.

Visual inspection of final cascades produced by the different methods is instructive and pictures of 100 keV, obtained using the software OVITO [22], are reproduced in figure 4. SDTrimSP produces cascades where the vacancies are generally concentrated inside the damaged zone while SIAs are found mainly around. In the MARLOWE cascades, remains of long replacement sequences along ⟨111⟩ directions are visible. MD cascades contain fewer defects and several MS-h cascades contain one large SIA loop while the MS-s shows smaller clusters.

Annealing of individual cascades have been done with our OKMC model, LAKIMOCA [8] based on the parameterization described in [23] at 473 K. We report here the statistic coming from annealing of each individual cascades in a 200 × 200 × 200 simulation box. The distributions of vacancy and SIA clusters as a function of their size are shown figure 5. The defects present in the box were summed to the

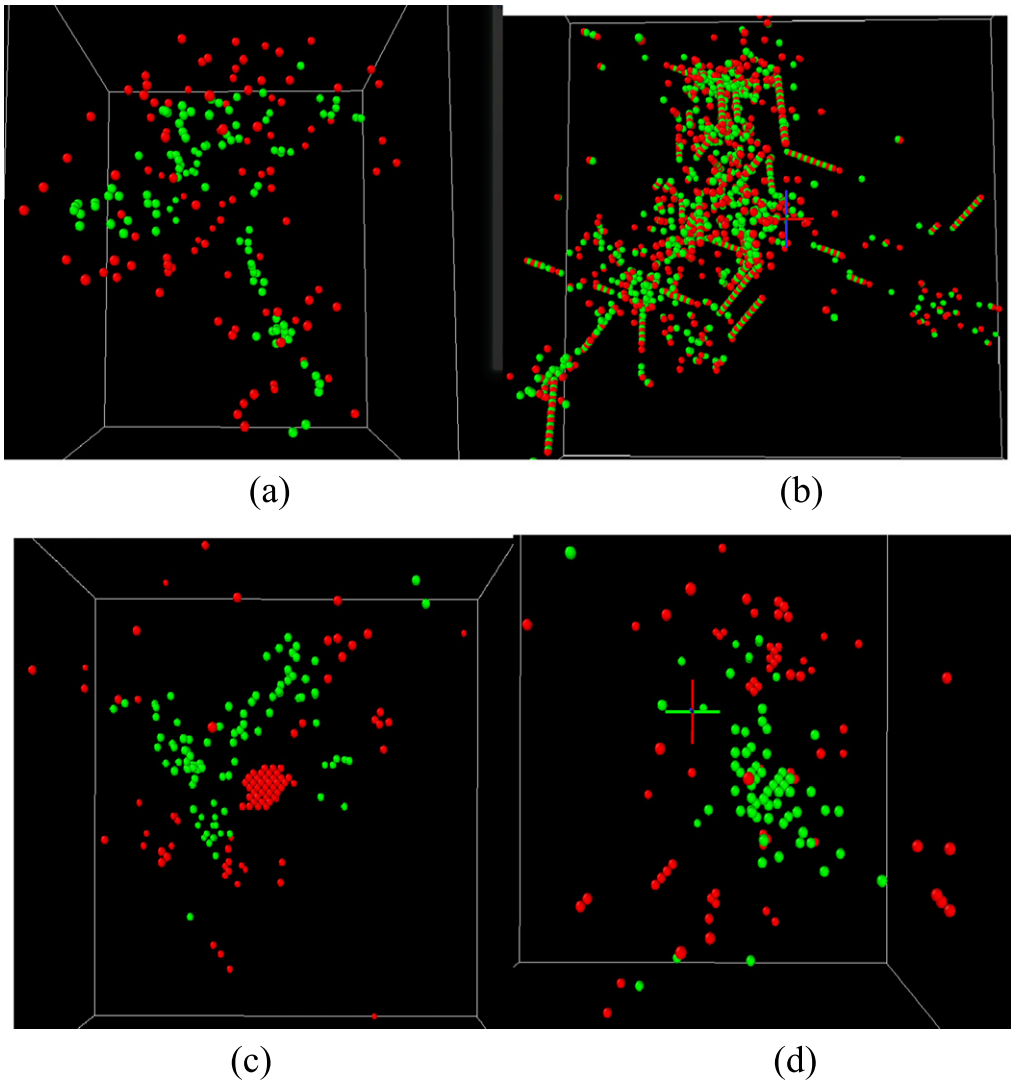

Figure 4. Pictures of 100 keV cascades using (a) SDTrimpSP + recomb, (b) Marlowe + recomb, (c) MD with MS-h and (d) MD with MS-s. Vacancies are in green and SIA in red, the sphere radius is the nearest neighbor distance and the boxes used for the illustration are typically 20 nm size.

ones that reached the surface of the box. This procedure gives the concentrations of defects that result from the intra-cascade interactions. It can be considered as the source term for larger scale models such as the mean field rate theory [24]. It is visible that SIA clusters are present in the MD cascades from the beginning and are much larger with the MS-h potential. During the annealing, the clusters grew significantly by accumulation of diffusing single SIAs. SIA clusters which were not present initially in SDTrimSP cascades formed during the annealing and their distribution follows a similar tendency. However, the sizes obtained never compare to the largest clusters of the MD cascades. The difference in the SIA cluster size distribution between MD and SDTrimSP is visibly reduced at the end of the annealing. At the investigated temperature, vacancies do not diffuse in W. During the annealing vacancy clusters mainly shrink by recombination with SIAs. A very small amount of vacancy clusters are reported in BCA cascades because of their concentration at the centered of the damaged region and further statistics are necessary to determine if the difference between MD and BCA is similar to the difference between MD cascades with the different potentials.

4. Conclusions

This work illustrates how a multiscale approach reveals some key aspects in the modeling of the damage produced by irradiation. We put in evidence a significant difference without and with the semi-core electrons in the DFT calculations of the TDE in particular in the $\langle 111 \rangle$ direction where we found respectively 44 eV and more than 80 eV. Furthermore, the variability of the TDE has been proven by MD runs illustrating the difficulty of addressing the quality of the empirical potential by comparing DFT and MD results. Work is in progress to further analyze the quality of empirical

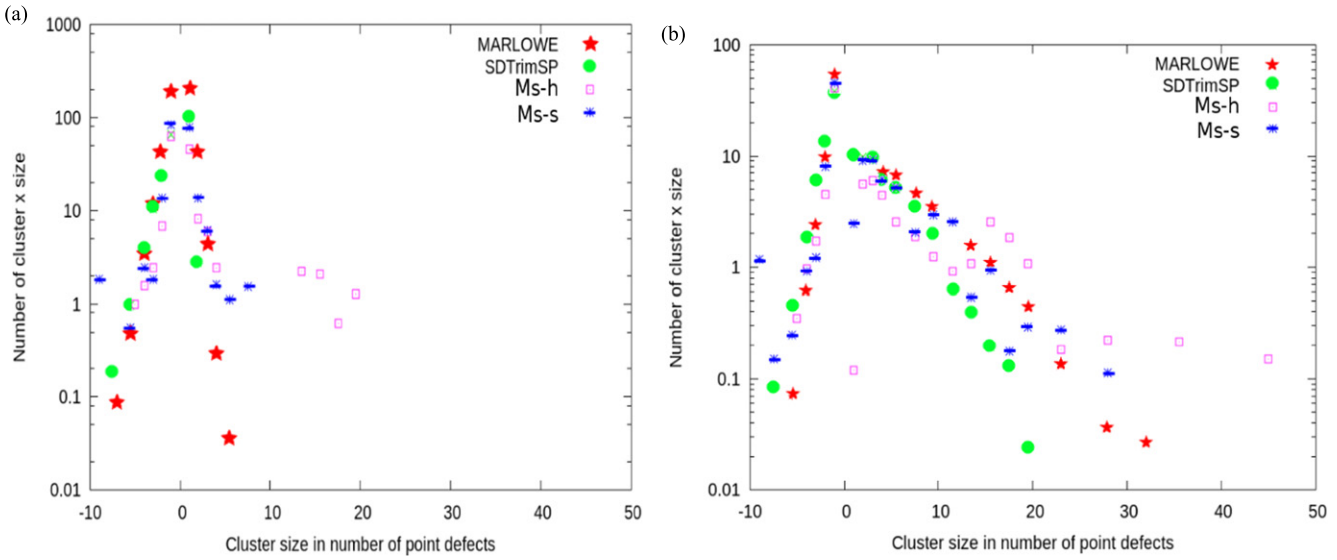

Figure 5. Averaged distributions of defect clusters (vacancy, resp. SIA, clusters are the negative, resp. positive, side of the *x* axis) after 0 s (a) and 10^{-6} s (b) of annealing of 100 keV cascades obtained with the different cohesive models, at 473 K using our OKMC model and parameterization, LAKIMOCA.

potential and link atomistic properties and defects produced in cascades.

Comparing MD and BCA cascades, the most appropriate value for the recombination distance is 12 Å, a larger value than the one we determined in our previous work [5] because of the use of bulk cascades instead of surface cascades, which contain more defects.

Another significant difference between BCA and MD cascades is the clustering of SIAs and vacancies in the latter. Our preliminary results showed that this difference is considerably reduced after the annealing of the cascade debris. The OKMC model should now be used along with other techniques such as mean field rate theory to investigate the long-term evolution at several temperatures which would allow comparison with experimental results.

Acknowledgments

This work was part-funded by the RCUK Energy Programme (grant number EP/I501045). This work has been carried out within the framework of the EUROfusion Consortium and has received funding from the Euratom research and training programme 2014–2018 under grant agreement No 633053. The views and opinions expressed herein do not necessarily reflect those of the European Commission. This work is supported by CEA under the collaborative contract number V 3542.001 on fusion engineering issues. This research has been done using the CRI supercomputer of the Université Lille1—Sciences et Technologies supported by the Fonds Européens de Développement Régional. This work contributed to the Enabling Research project on tritium retention in controlled and evolving microstructure.

References

[1] Sand A E, Dudarev S L and Nordlund K 2013 *Europhys. Lett.* **103** 46003
[2] Mutzke A, Schneider R, Eckstein W and Dohmen R 2011 *SDTrimSP: Version 5.00.* Report IPP 12/8 Max-Planck-Institut für Plas maphysik, Garching, Germany
[3] www.srim.org
[4] RSICC Home Page (https://rsicc.ornl.gov/codes/psr/psr1/psr-137.html) (accessed May, 2014)
[5] Hou M, Ortiz C J, Becquart C S, Domain C, Sarkar U and De Backer A 2010 *J. Nucl. Mater.* **403** 89
[6] Stoller R E 2002 *J. Nucl. Mater.* **307** 935
[7] Nordlund K, Keinonen J, Ghaly M and Averback R S 1999 *Nature* **398** 49
[8] Domain C, Becquart C S and Malerba L 2004 *J. Nucl. Mater.* **335** 121
[9] Blöchl P E 1994 *Phys. Rev.* B **50** 17953
[10] Kresse G and Joubert D 1999 *Phys. Rev.* B **59** 1758
[11] Perdew J P *et al* 1992 *Phys. Rev.* B **46** 6671
[12] Kresse G and Hafner J 1993 *Phys. Rev.* B **47** 558
Kresse G and Hafner J 1994 *Phys. Rev.* B **49** 14251
Kresse G and Furthmüller J 1996 *Comput. Mater. Sci.* **6** 15
Kresse G and Furthmüller J 1996 *Phys. Rev.* B **54** 11169
[13] Olsson P and Domain C 2010 *Proc. Int. Conf. Multiscale Materials Modeling, 5th* (*Freiburg, Germany*) p 4
[14] Marinica M-C, Ventelon L, Gilbert M R, Proville L, Dudarev S L, Marian J, Bencteux G and Willaime F 2013 *J. Phys.: Condens. Matter* **25** 395502
[15] Ziegler J F, Biersack J P and Littmark U 1985 *The Stopping and Range of Ions in Solids* (New York: Pergamon) (www.srim.org)
[16] Nordlund K, Wallenius J and Malerba E L 2006 *Nucl. Instrum. Methods Phys. Res.* B **246** 322
[17] Eckstein W 1991 *Computer Simulation of Ion–Solid Interactions* (*Springer Series in Materials Science* vol 1) (Berlin: Springer)
[18] Ortiz C J, Souidi A, Becquart C S, Domain C and Hou M 2014 *Radiat. Eff. Defects Solids* **169** 592
[19] Souidi A, Elias A, Djaafri A, Becquart C S and Hou M 2002 *Nucl. Instrum. Methods Phys. Res.* B **193** 341

[20] Hou M, Souidi A and Becquart C S 2002 *Nucl. Instrum. Methods Phys. Res.* B **196** 31
[21] Scholz A and Lehmann C 1972 *Phys. Rev.* B **6** 813
[22] Stukowski A 2010 *Modelling Simul. Mater. Sci. Eng.* **18** 015012
[23] Becquart C S, Domain C, Sarkar U, De Backer A and Hou M 2010 *J. Nucl. Mater.* **403** 75
[24] Jourdan T and Crocombette J-P 2013 *Phys. Rev.* B **86** 054113